Colicin-mediated transport of DNA through the iron transporter FepA

Ruth Cohen-Khait[1†], Ameya Harmalkar[2†], Phuong Pham[1], Melissa N. Webby[1], Nicholas G. Housden[1], Emma Elliston[1], Jonathan TS. Hopper[3], Shabaz Mohammed[1], Carol V. Robinson[3], Jeffrey J. Gray[2*] and Colin Kleanthous[1*]

Author Address

1. Department of Biochemistry, University of Oxford, UK
2. Chemical & Biomolecular Engineering, Johns Hopkins University, USA
3. Department of Chemistry, University of Oxford, UK

KEYWORDS *Macromolecules transport | Bacteriocin | Outer membrane | Conformational changes | Rosetta flexible backbone docking*

ABSTRACT

Colicins are protein antibiotics used by bacteria to eliminate competing Escherichia coli. A key event in the selective colicin function is a highly specific initial recognition step of an outer membrane (OM) receptor, which consequently allows the active transport of the colicin across the otherwise impervious OM. Though the colicin-receptor interaction is exclusive, the translocation process is likely to be universal as many receptors and colicins have surprisingly similar 3D folds. Here, using a combination of photo-activated crosslinking, mass spectrometry, and structural modeling, we reveal how colicin B (ColB) associates with its OM receptor FepA. We demonstrate that complex formation is coincident with a large-scale conformational change in the colicin. In vivo crosslinking experiments and further simulations of the translocation process indicate that part of the colicin engages active transport by disguising itself to part of the cellular receptor. Applying live-cell fluorescence imaging we were able to follow ColB into E. coli and localize it within the periplasm. Finally, we demonstrate that single-stranded DNA coupled to ColB is transported into the bacterial periplasm, emphasizing that the import routes of colicins can be exploited to carry large cargo molecules into Gram-negative bacteria.

Bacteria are the most common and diverse form of life on earth. The remarkable abundance of different bacterial strains and species capable of surviving at almost any environment frequently leads to severe inter-bacterial competition over space and limited resources[1]. The recurrent need to compete for basic life necessities has led the evolution of inter-bacterial weapons. Bacterial weapons are usually toxins which either perform a nuclease activity[2] (e. g., DNase, RNase, or tRNase) or destruct the cellular membrane integrity[3] (e. g., pore forming proteins or enzymes such as amidase, lipase and peptidoglycan hydrolase). The most challenging step in this antibiotic bacterial war is to specifically deliver the toxin to the closely related competing bacterial strain while avoiding self-killing. Immunity proteins expressed alongside the toxin inactivate the cytotoxic activity within the producing strains[4]. Cytotoxic proteins can be delivered either in a contact-dependent manner, targeting neighboring cells relying on the assembly of supramolecular secretion machineries[5], or in a way which does not depend on physical contact between the cells as exemplified by bacteriocins[6]. Colicins are bacteriocins that are specifically active against *E. coli*. Colicin production is tightly regulated by the cellular SOS response as the only manner by which colicins are released to the environment is upon lysis of the colicin producing cell[7]. The key obstacle colicins face prior to executing their killing action is penetrating the impermeable bacterial cellular envelope[8]. The cellular envelope of gram negative bacteria (such as *E. coli*) is composed of the asymmetric non-energized outer-membrane (OM) (containing lipopolysaccharides at the outer leaflet and phospholipids in the inner leaflet), the symmetric energized phospholipidic inner-membrane (IM) and the intervening peptidoglycan containing periplasm[9]. Moreover, colicins are large (29-75 kDa) proteins that cannot spontaneously diffuse through the cellular envelope[10], hence they also face the challenge of finding active transport into the cell, foremostly the OM[11]. There are two structurally related energy transfer systems that are exploited by colicins to traverse the OM barrier: 1) The Tol system, which stabilizes the

OM during cellular division composed of the IM Tol Q/R/A complex and the periplasmic TolB and Pal[12], and 2) the Ton system composed of the IM protein complex TonB-ExbB-ExbD, which is mainly responsible for the active import of nutrients through specialized OM receptors[13]. Most of a colicin's structure is involved in overcoming the translocation impediments across the cellular envelope. Colicin proteins are usually composed of three major structural domains: 1) a central receptor binding domain (R) 2) an N-terminal translocation domain (T) and 3) a C-terminal cytotoxic domain[14]. The main purpose of the receptor binding domain is to interact with a specific receptor (usually a nutrient transporter) in the OM and to anchor the colicin to the cell. Once the colicin is in position the T domain interacts with a different OM protein, upon which the colicin translocation is dependent[15,16]. Colicin B (ColB) is a pore forming toxin that is one of the earliest colicins to be described[17]. However, little is known about the cellular translocation process of ColB beyond its dependence on the OM ferric enterobactin transporter FepA, and the Ton system[18]. No additional proteins have been identified for ColB toxicity, which may explain why, unlike most other colicins, ColB is composed of only two functional domains: an N-terminal domain that serves as both a receptor binding domain and a translocation domain (herein referred to as the ColB RT domain) and a pore forming C-terminal cytotoxic domain[19]. The ColB receptor FepA is a 22-stranded β-barrel TonB-dependent transporter (TBDT) with an N-terminal plug domain blocking its lumen[20 21,22]. Here, we have investigated how ColB interacts with FepA and exploits it for its active transport into the cell. We have then further examined whether ssDNA cargo could hitchhike ColB into bacterial cells. We have applied a unique approach combining *in vitro* and *in vivo* photoactivated crosslinking, mass-spectrometry, and structural modeling with Rosetta to follow the key stages in ColB-FepA association process. We identify an energetically favorable encounter complex that induces major conformational changes in the colicin and consequently leads to the formation of a stable complex *in vitro*. Following further *in vivo* crosslinking data with additional structural modeling, we identify an intermediate TonB dependent translocation state. We show how the partially unstructured N-terminal 55 amino acids of the colicin replace the N-terminal half plug domain of the receptor, which is actively unfolded by TonB. This ultimately allows direct engagement of the colicin with the periplasmic energy transferring agent. Furthermore, applying fluorescence microscopy we exhibit the direct visualization of translocated ColB RT domain in the periplasm of *E. coli*, demonstrating unambiguously that translocation requires only FepA and TonB. Finally, we show that the active transport mechanism for ColB through FepA can be exploited to deliver ssDNA into the cell.

Receptor binding induces large-scale conformational changes in ColB

ColB RT shares 96% sequence similarity with the N-terminal domain of colicin D (ColD) and thus is believed to take a similar route into the cell. However as ColD is a tRNase its cytotoxic domain needs to further be delivered into the cytoplasm (while the periplasm is the destination of the pore forming ColB). Though it is known that both ColB and ColD depend on FepA and TonB for their cellular penetration it is not yet clear how these colicins exploit this system for translocation. FepA is the only identified OM contact of ColB, as Cir is the only OM contact of ColIa. A stoichiometric complex ratio of 2:1 has been detected for the Cir-ColIa complex respectively suggesting that ColIa attaches to the OM via one Cir copy and translocates via another[23]. We applied advanced native state mass-spectrometry to examine the stoichiometric complex ratio of the FepA-ColB complex, assembled *in vivo* on *E. coli* surface. Unlike Cir-ColIa, we found the FepA-ColB complex ratio is 1:1 (Extended data Fig. 1), in agreement with the conclusion drawn from previous studies *in vivo*[24]. Thus, it appears that ColB associates and translocates via a single copy of FepA.

The FepA-ColB interaction occurs via two common protein folds: FepA like many other OM transporters is a 22 stranded β-barrel with a globular N-terminal plug domain[25]. ColB RT belongs to the pyocin_S domain superfamily[26], a 3D protein fold that is very common amongst bacteriocins with nuclease cytotoxic activity and is usually associated with translocation across the IM. ColB is the only known example of a pore forming colicin exhibiting the pyocin_S domain, which apparently uses this fold to translocate across the OM. The high structural similarities FepA and ColB RT share with other OM transporters/colicin domains is emphasized in Extended data Fig. 6. Regardless of the common 3D folds, the FpeA-ColB complex is highly specific (Fig. 3a)[27,28]. Here we applied Rosetta based structural simulations to determine how the ColB RT domain associates with FepA. We examined the available PDB structures of ColB[29] (PDB 1RH1) and FepA[20] (PDB 1FEP) applying a Rosetta docking algorithm[30], which revealed a clear energy funnel (Fig. 1d) for an encounter complex (EC) structure (Fig. 1a). Despite the FepA-ColB complex crystallization attempts being thus far unsuccessful we were able to back up the Rosetta model predictions applying a *pBPA* crosslinking approach. We introduced P-benzoyl-L-phenylalanine (*pBPA*) mutations on unique ColB RT surface loops, previously highlighted as potential FepA binding sites[31] (Extended data Fig. 2). Exposure to UV (365 nm) results in *pBPA* non-specific crosslinking to a carbon atom within ~4 Å[32]. We executed photoactivated crosslinking experiments both *in vitro* using the OM protein fraction as a FepA source, or *in vivo* on live *E. coli* cells. We identified crosslinks on SDS-gels and further analyzed them by LC MS-MS, as previously described in White et al[33]. Applying this method, we identified 3 crosslinks *in vitro* – two of which (ColB 202 & 205 with FepA 642 & 639 respectively) supported the initial EC computed with Rosetta (Fig. 1a, Supplementary Fig. 3a, Supplementary Fig. 4a-c). Thus, recent progress in the Rosetta docking energy function[30,34] allowed the accurate prediction of the EC (Fig 1a) as has been further confirmed by *pBPA* crosslinking experiments (Fig. 1, Extended data Fig. 3a, Extended data Fig. 4a-c). However, the third crosslink (ColB 55 with FepA 652) yet remained to be explained.

ColB 55 appears in close proximity to ColB 202 & 205 on the ColB PDB structure, yet our crosslinking data show

that it does not crosslink to neighboring residues on the receptor – suggesting that complex formation induces conformational changes within the colicin (Fig. 1b). In order to improve the structural model of the ColB-FepA complex, we stimulated the partially unstructured N-terminal tail of ColB (residues 1-55) as a 'floppy tail`, allowing it to sample its environment freely[30]. The resulting model of the stable complex (SC) explains all three *in vitro* observed crosslinks (Fig. 1c) and seems to be energetically favorable over the initially calculated EC (Fig. 2d, Movie 1). The calculated SC seems to also bring the ColB TonB box closer to the FepA lumen (Fig. 1c).

Previous studies have emphasized the importance of the FepA surface loops in substrate recognition and have further indicated the sequential order of the loops movement upon substrate binding[35-37]. Here we did not account for possible energetically favorable movements of the FepA surface loops because our experimental data focused on the binding colicin, and the manner it exploits FepA for active transport into the cell. Moreover, the mapped crosslinking area on FepA has not been previously identified as vital for the ColB-FepA interaction. It is possible that ColB binding induces movement in the surface loops of FepA in a similar manner to ferric enterobactin, which may slightly alter the final *in vitro* SC structure (Fig. 1c). However, it is unlikely to change our main structural conclusions regarding the initial FepA-ColB recognition step EC (Fig. 1a), the induced conformational changes in ColB (Fig. 1b, Fig. 1c) and the essence of the proposed first translocation step across the FepA lumen (Fig. 2a). The combination of Rosetta based structural modeling and *pBPA* crosslinking identified the nature of the previously reported biphasic association process of the ColB-FepA complex (Fig. 1, movie 1)[24].

ColB exploits FepA for its active translocation into the cell

The route of ColB translocation in a FepA dependent manner is unknown. It has been proposed that ColB passes through the FepA lumen[18], this hypothesis has been supported by the partial dislocation of the FepA half plug domain demonstrated by exposure to periplasmic Cys labelling[18,38]. On the other hand when a different Cys label was used it appeared that ColB binding induced no conformational changes in the FepA plug domain, implying that ColB probably does not penetrate the cell through FepA[39]. Here we show how the partially unstructured flexible N-terminal tail of ColB (residues 1-55) occupies the TonB dependent channel generated by the FepA half plug domain unfolding (Fig. 2). We suggest that while complex formation (Fig. 1) is a highly specific step, the translocation mechanism through 22 stranded beta-barrel TBDTs is likely to be applicable to many other systems sharing similar protein folds (Extended data Fig. 6). We identified the three crosslinks observed *in vitro* also *in vivo* as well as additional two crosslinks which we further mapped by LC MS-MS (Extended data Fig. 3b, Extended data Fig. 4d-e). The additional two crosslinks did not form in the absence of the energy transferring agent TonB (Extended data Fig. 3c).

The TonB box is a conserved penta-peptide sequence essential for interaction with TonB[40], and thus is expected to lead the colicin translocation course. Two essential TonB boxes participate in the ColB translocation process: one on the colicin itself and the other on its OM receptor FepA [18,41]. We examined the ability of the *in vivo* observed ColB 81-FepA 214 crosslink to form as a function of both the FepA and ColB TonB boxes. The ColB 81-FepA 214 does not form in the absence of the FepA TonB box, but it still forms in the absence of the ColB TonB-box (Fig. 2b). Hence, as both TonB boxes are essential for full colicin translocation, the ColB 81-FepA 214 crosslink appear to capture a stable intermediate translocation step. These experiments were not performed on the second *in vivo* identified crosslink ColB 19-FepA 58 as ColB 19 is already part of the ColB TonB box.

For the FepA homologous vitamin B_{12} transporter BtuB, Hickman et al[42]. showed that the N-terminal globular plug domain of the receptor is composed of two mechanically independent half-plug domains, with the N-terminal half plug more likely to unfold due to TonB applied force[42]. This model has also previously been proposed for the TonB dependent pyocin S2 translocation mechanism via FpvAI[33]. In order to investigate the structures during the dynamic translocation process, we applied Rosetta to stimulate the unfolding of the N-terminal half (residues 1-74) of the globular FepA plug domain as previously demonstrated on BtuB[42]. We stimulated the ColB-FepA translocation process starting with the computed SC structure (Fig. 1c) and using the *in vivo* identified crosslinks as guides to generate three intermediate structures in 4 Å increments (Fig. 2a, Fig. 2c). The stimulated structures indicate that the translocating N-terminal ColB tail (residues 1-55) occupies the cavity generated by the FepA half plug removal with the ColB TonB box now positioned in place of the former FepA TonB box (Fig. 2a, Fig. 2c). Hence it appears that there are two independent energy transfer events essential for the colicin translocation: at first TonB induces unfolding of the N-terminal FepA half plug domain bringing the ColB TonB-box into the periplasm (Fig. 2c), waiting for a yet another encounter with TonB which would enable complete translocation of the colicin. The computed model (Fig. 2c) supports the previously proposed model for TonB dependent bacteriocin translocation developed using Pyocin S2 translocation via FpvAI[33] emphasizing the importance of the two independent encounters with the energy transferring agent TonB: The first receptor mediated encounter allows the translocation of the bacteriocin's TonB box into the periplasm (Fig. 2c) in a wait for a second encounter which will allow the active colicin translocation into the cell. The computed model indicates how the N-terminal tail of the translocating colicin mimics the unfolded receptor half-plug domain replacing the receptor's TonB box with the colicin's one (Fig. 2a, Fig. 2c).

ColB can transport ssDNA through FepA

The OM is the foremost barrier into the cell which due to its low permeability provides gram negative bacteria with protection against a various range of antibiotics[43]. A recently developed antibiotic delivery strategy termed 'The Trojan Horse` relies on antibiotic molecules conjugation to siderophores which are actively consumed by bacteria due to bacterial innate need for iron ions[44,45]. As we have ascertained the route through which the ColB RT domain bypasses the OM we now addressed the question of whether other types of molecules

could be transported into bacteria by piggy-backing the colicin?

As a first step we examined whether the ColB RT domain could be followed into bacterial cells. We have conjugated the ColB RT domain (residues 1-341) to a small fluorescent dye (Alexa 488 nm) and applied live-cell fluorescence microscopy to examine its ability to penetrate into *E. coli* cells, as well as determine its cellular localization (Fig. 3a). We defined cellular penetration as a fluorescent signal resistant to trypsin treatment. Deletion of the ColB TonB box (residues 17-21) resulted in a complete loss of the colicin's ability to translocate, however it has maintained its ability to bind FepA (Fig. 3a). No binding was detected in FepA knock out cells (Fig. 3a). Consistent with ColB being a pore forming colicin, the fluorescent signal was lost upon cellular spheroplasting (disruption of the OM and the periplasmic peptidoglycan layer) suggesting that ColB RT remained in the periplasm and did not translocate into the cytoplasm (Fig. 3a). In order to examine whether colicins could be used to deliver macromolecules into the cell in a similar way to siderophores we generated fluorescent colicin-DNA fusions. We used maleimide conjugation to attach fluorescent ssDNA (15A or 5A 10C) to an introduced C-terminal Cys on ColB RT. We verified that the fluorescent signal followed the attached DNA molecule by exposing it to DNase treatment (Extended data Fig. 5). Hence, any translocated fluorescent signal indicated that the conjugated DNA molecule has transferred into the cell. The fluorescent signal appeared to follow the ColB RT periplasmic localization in a FepA dependent manner (Fig. 3b). In order to test whether dsDNA could follow the colicin's path into the cell the ColB RT 5A 10C construct was incubated with a 10G DNA fragment. The addition of the 10G fragment did not disrupt the construct's ability to translocate (Fig. 3b). However, it is not clear whether the dsDNA has fully translocated into the cell, or whether the applied force (due to TonB activity) has disrupted the dsDNA – so that only the conjugated 5A 10C fragment has translocated in. The colicin-DNA conjugation experiments highlight that colicin translocation domains can be utilized to transport non-protein macromolecules through the OM barrier. It also emphasizes the sturdiness of the TonB/ExbB/ExbD system dependent colicin transport process and offer a highly specific (protein-protein interaction mediated) method for DNA delivery into bacteria.

Conclusions

Here we show that the translocation process of ColB is a dynamic process that involves receptor mimicry and relies on two energy transfer events. The approach described here, combining photoactivated crosslinking and structural modeling enabled a detailed characterization of the cascade of complex readjustment events that drive colicin transport across the OM. The described translocation mechanism likely applies to other FepA and TonB dependent toxins such as ColD and phage H8[46]. Moreover, the defined mechanism is also relevant to other bacteriocins utilizing TBDTs with similar folds. The emphasized ability of bacteriocin-DNA conjugations to follow the colicin route into the cell opens a large range of opportunities to utilize bacteriocins for bypassing the otherwise strictly impermeable gram-negative bacterial OM. This includes development of novel antibiotics delivery strategies in a similar way to siderophores (of which colicins are natural mimics). It also applies to the area of genomic manipulations in non-domesticated bacteria, as the colicin-DNA fusions provide a highly specific manner of targeted DNA delivery into bacteria.

Materials and Methods

Protein expression and purification

All colicin constructs were conjugated to a 6xHis tail at their C-terminus and cloned at the second multiple cloning site of the apACYCDuet-1 (Novagen) plasmid where they were expressed under a T7 promotor. The plasmids were transformed into BL21(DE3) *E. coli* cells. Transformed cells were grown at 37° C in Lysogeny Broth (LB) media pH 7.2 while shaking at 180 rpm to OD_{600}~0.6 at which point 1 mM Isopropyl-D-thiogalactopyranoside (IPTG) was added and the temperature was reduced to 20° C for an overnight incubation. The protein has been eluted as described in Khait and Schreiber (2012)[47]. Briefly, protein expressing cells were re-suspended in 20 mM Tris pH 7.5, 0.5 M NaCl, 5 mM Imidazole and sonicated (Sonicator 4000: 70%, 1.5 min, 3 sec on:7 sec off). The sonicated cellular extract was spun down and the supernatant has been incubated with His-binding resin (Merck 69670-5) for 10-30 min at room temperature. The Ni-resin and the bound protein were then gently (1000 g <) spun down, washed three times and re-suspended in the same buffer containing 0.5 M Imidazole which allowed protein elution. The protein has been dialyzed to PBS at 4° C overnight. FepA has been expressed on a pBAD/Myc-HisB (Novagen) plasmid, transformed into either Bl21(DE3) or BW25113 ΔFepA (JW5086-3) *E. coli* cells. FepA has been expressed similarly to the colicin proteins except of the LB growing media pH being 6.12 and protein expression induction with 0.15% L-Arabinose. The FepA containing protein OM fraction has been purified as previously described for ompF[48]. Protein concentrations were determined through absorbance at 280 nm using a sequence-based extinction coefficient.

Fluorescent protein labelling

Colicins were conjugated to Alexa 488 or 15 b DNA – Alexa 488 by maleimide reactions as described in Kleanthous et al[49] with some adaptions: the purified protein was incubated with 10 mM DTT for one hour at room temperature (or overnight at 4° C) it was then run throw a desalting column (buffer: 25 mM Tris pH 7.5, 100 mM NaCl) and immediately incubated with x1.1 or x3 ratio of Eurogentech maleimide DNA conjugates or maleimide Alexa 488 respectively for one hour at room temperature, the reaction was terminated by the addition of 5 mM DTT. The protein has been desalted again, retrieved by Ni-beads as in the previous section and dialyzed to PBS. The efficiency of the fluorescent conjugations has been determined on a fluorimeter (UV/VIS V-550 Jasco). The protein-DNA conjugation sensitivity to DNase and trypsin treatments has been analyzed on 15%-SDS page gels.

Native State Electrospray Ionization Mass-spectrometry

Sixty mg of ColB RT (341 aa) were added to a 5 L culture of BW25113(ΔFepA) cells over expressing FepA from a pBAD/Myc-HisB (Novagen) plasmid. The complex has been purified following the protocol previously described for ompF[48]. A 5 ml HiTrap desalting column (GE Healthcare) was used to exchange the complex buffer into 100 mM ammonium acetate, 1% (w/v) β-OG, pH 6.9. Mass spectrometry measurements were made from a static nanospray emitter, using gold-coated capillaries prepared in-house[50], on a quadrupole time-of-flight mass spectrometer (Micromass) modified for high mass transmission. Liberation of the protein complex from β-OG detergent required energetic instrument parameters and the low m/z region of spectra where dominated by detergent clusters. Operating conditions used include capillary voltage 1800V, sample cone 200V, extractor 10V, collision cell energy 140-200V, source backing pressure 5.92 x10-3 mbar and Argon collision cell pressure 3.5 – 5 MPa.

Crosslinking

The crosslinking procedure was similar to White et al (2017)[33]. In short *pBPA* mutations were introduced at 21 different positions of ColB RT (341 aa) GFP. For *in vitro* crosslinking 1 μM of *pBPA* containing colicin was incubated with 1 ml of an OM protein fraction (in PBS pH=6.5, 5 mM EDTA, 2% β-OG) extracted from BW25113 FepA knock-out cells over expressing FepA containing ~1 μM FepA and exposed to UV light (365 nm) for 1 hour at 4° C. The colicin and bound/crosslinked FepA were then extracted by EDTA resistant Ni-beads cOmplete (Merk). For *in vivo* crosslinking the colicin was incubated with 800 ml cells over expressing FepA overnight at 20° C. The *pBPA* containing colicin was added to the LB media (pH 6.12) and incubated for 90 min at 37° C while shaking. The cells were then spun down, colicin excess was washed with 50 ml PBS, the cells were re-suspended in 10 ml PBS and exposed to UV light (365 nm) for 1 hour at 4° C. The cells were then re-suspended in 10 mM Tris pH 8, 0.25 % lithium diiodosalicylic acid (LIS), 2% Triton x100, sonicated, the cell debris were spun down, and the supernatant ultra-centrifuged (200,000 × g for 45 min 4° C) the pellet was re-suspended in PBS pH=6.5, 5 mM EDTA, 2% n-octyl-β-D-glucopyranoside (β-OG), ultracentrifuged again – and the colicin with its bound/crosslinked proteins was extracted by EDTA resistant Ni-beads cOmplete (Merk). The extracted proteins were run on 12%-SDS page gels, GFP fluorescent bands of adequate size were analyzed by LC MS/MS for crosslinking mapping.

LC MS/MS crosslinking analysis

Peptides were separated on an EASY-nLC 1000 ultra-high-performance liquid chromatography (UHPLC) system (Proxeon) and electrosprayed directly into a Q Exactive mass spectrometer (Thermo Fisher). Peptides were trapped on a C18 PepMap100 pre-column (300 μm inner diameter × 5 mm, 100 Å pore size, Thermo Fisher) using solvent A [0.1% (v/v) formic acid in water] at 500 bar and then separated on an in-house packed analytical column (50 cm × 75 μm inner diameter packed with ReproSil-Pur 120 C18-AQ, 1.9 μm, 120 Å pore size, Dr. Maisch GmbH) with a linear gradient from 10% to 55% (v/v) solvent B [0.1% (v/v) formic acid in ACN] in 45 min at 200 nL/min. Full scan MS spectra were acquired in the Orbitrap (scan range 350-2000 m/z, resolution 70,000, Automatic Gain Control target 3e6, maximum injection time 100 ms). After the MS scans, the 10 most intense peaks were selected for Higher-energy collisional dissociation (HCD) fragmentation at 30% of normalized collision energy. HCD spectra were also acquired in the Orbitrap (resolution 17,500, Automatic Gain Control target 5e4, maximum injection time 120 ms) with first fixed mass at 100 m/z. Charge states 1+ and 2+ were excluded from HCD fragmentation. MS data searched using the pLink software[51]. The database contained the target proteins and common contaminants. Search parameters were as follows: maximum number of missed cleavages = 2, fixed modification = carbamidomethyl-Cys, variable modification 1 = Oxidation-Met, variable modification 2 = Glu to pyro-Glu. Crosslinking from D to K, S, T or N-terminus was considered. Data were initially filtered to a False-discovery rate (FDR) of 1%. Crosslinks were further filtered/inspected with specific emphasis on fragmentation patterns.

Structural modeling

Note: EC (Encounter Complex), SC (Stable Complex)

Computational modeling of the FepA-ColB interaction

Structure preparation. The crystal structures of ColB (1RH1[29]) and FepA (1FEP[20]) were used as starting templates for the computational modeling. Because the crystal structures were missing key loops needed to effectively propagate backbone motions, we added these loops (residues 31-44 on ColB, 323-335 and 384-40 on FepA) using SWISS MODELLER[52]. To eliminate energetically unfavorable side-chain or backbone clashes, we then relaxed the structures using constraints to the native crystal coordinates using RosettaRelax[53].

Stage 1: Modeling the semi-rigid encounter complex (EC)

We determined putative local binding conformations by first performing rigid-body global docking using Rosetta's RepliaDock2 protocol (built upon prior work on temperature and Hamiltonian replica exchange Monte Carlo approaches[54,55]) and clustering the lowest energy docked structures. Then starting from each low-energy structure, we refine the structures in a local binding region by using our RosettaDock4.0[56] protocol that adaptively swaps receptor and ligand conformations from a pre-generated ensemble of structures. We diversify the backbone conformations in the ensemble by using: (1) ReplicaDock 2.0 (2) Rosetta Relax[53] and (3) Rosetta Backrub[57]. Local docking generates ~6,000 decoys, which are scored based on their interface energies, defined as the energy difference between the total energy of the complex and the total energy of the monomers in isolation (see Extended data for detail and command-lines).

Stage 2: Modeling the stable complex (SC) allowing backbone flexibility

To explore the possibility of ColB flexible N-terminal domain (residues 1-55) interacting explicitly with FepA, we used the Rosetta FloppyTail[58] algorithm, which allows modest sampling of backbone degrees of freedom following a two-stage approach. First, in the low-resolution stage, side-chains are

represented by a centroid atom and the backbone conformational space is extensively sampled. Then, in the high-resolution stage, all side-chain atoms are returned to refine the structures. We generated ~5,000 hypothetical decoys starting from the encounter complex obtained in Stage 1 (EC). The 5,000 perturbation cycles and 1,000 refinement cycles were used for each decoy. To direct the MC sampling of the FloppyTail algorithm toward possible interacting regions, atom-pair constraints based on the experimental (*in vitro*) crosslinking residues guided the search. These constraints were calculated based on a "harmonic" potential with a mean of 6 Å and a standard deviation set to 0.25 Å between the Cα atoms of the candidate residues. Each output decoy was further relaxed to remove unfavorable clashes, and the 100 top-scoring models were then docked using RosettaDock4.0[56] using a fixed backbone. Translational and rotational moves were performed on the top models to generate ~5,000 docking decoys. To confirm the feasibility of these decoys, we evaluated the interface energies and compared the energy landscape of decoys in Stage 2 with the prior decoys obtained in Stage 1 (Fig. 1c).

Stage 3: Prediction of the translocation pathway applying in vivo crosslinking data

Following the partial unfolding of the plug domain in the related TonB-BtuB system[42], we allowed backbone movement in the FepA 75-residue half-plug domain (residues 1-75) and the ColB flexible N-terminal domain (residues 1-43). Since simulating the dynamic unfolding of FepA half-plug with simultaneous translocation of the ColB via the barrel protein would be intensely demanding computationally, we instead create models to represent three steps along the dynamic pathway of the unfolding-translocation process. A figure showing the workflow with intermediate snapshots and complete details of each phase of our three-part model creation are given in the Extended data computational methods. Briefly, to create each structure along the pathway, we (1) displace the FepA half-plug (residues 1-75) using Rosetta FloppyTail to pull the terminus out by 4, 8, and 12 Å, respectively, to begin making each of the three structural steps in the pathway; (2) translocate the ColB N-terminal domain (residues 1-43) using both *in vitro* and *in vivo* crosslinking constraints with Rosetta FloppyTail; and (3) refine both FepA and ColB conformation and rigid-body displacement using RosettaDock with a flexible FepA half-plug and ColB N-terminal domain. During stages (1) and (2), backbone motions in FloppyTail are propagated toward the closest terminus, but in stage (3), ColB backbone perturbations during docking are propagated back toward the bulk of ColB to facilitate it finding the optimal rigid-body displacement while the N-terminal domain is translocating. Finally, we calculate interface scores to reveal the favorability relative to conformations of other models presented in this paper along the hypothesized unfolding-translocation pathway (Extended data Fig. 7).

AUTHOR INFORMATION

* Correspondence To: Colin Kleanthous colin.kleanthous@bioch.ox.ac.uk, Jeffrey J Gray jgray@jhu.edu

† Equal author contribution

Funding Sources

The experimental work was funded by a BBSRC grant BB/P009948/1. AH and JJG were funded by the U.S. National Institutes of Health grant R01-GM078221.

REFERENCES

1 Hibbing, M. E., Fuqua, C., Parsek, M. R. & Peterson, S. B. Bacterial competition: surviving and thriving in the microbial jungle. Nature Reviews Microbiology 8, 15-25, doi:10.1038/nrmicro2259 (2010).

2 Aoki, S. K. et al. A widespread family of polymorphic contact-dependent toxin delivery systems in bacteria. Nature 468, 439-442, doi:10.1038/nature09490 (2010).

3 Montville, T. J. & Bruno, M. E. C. Evidence that dissipation of proton motive force is a common mechanism of action for bacteriocins and other antimicrobial proteins. International Journal of Food Microbiology 24, 53-74, doi:https://doi.org/10.1016/0168-1605(94)90106-6 (1994).

4 Papadakos, G., Wojdyla, J. A. & Kleanthous, C. Nuclease colicins and their immunity proteins. Quarterly reviews of biophysics 45, 57 (2012).

5 Green, E. R. & Mecsas, J. in Virulence Mechanisms of Bacterial Pathogens 213-239 (2016).

6 Simons, A., Alhanout, K. & Duval, R. E. Bacteriocins, Antimicrobial Peptides from Bacterial Origin: Overview of Their Biology and Their Impact against Multidrug-Resistant Bacteria. Microorganisms 8, 639 (2020).

7 Cascales, E. et al. Colicin Biology. Microbiology and Molecular Biology Reviews 71, 158-229, doi:10.1128/mmbr.00036-06 (2007).

8 Kleanthous, C. Swimming against the tide: progress and challenges in our understanding of colicin translocation. Nature reviews. Microbiology 8, 843-848, doi:10.1038/nrmicro2454 (2010).

9 Masi, M., Réfregiers, M., Pos, K. M. & Pagès, J.-M. Mechanisms of envelope permeability and antibiotic influx and efflux in Gram-negative bacteria. Nature Microbiology 2, 17001, doi:10.1038/nmicrobiol.2017.1 (2017).

10 Braun, V., Pilsl, H. & Groß, P. Colicins: structures, modes of action, transfer through membranes, and evolution. Archives of Microbiology 161, 199-206, doi:10.1007/BF00248693 (1994).

11 Egan, A. J. F. Bacterial outer membrane constriction. Molecular Microbiology 107, 676-687, doi:https://doi.org/10.1111/mmi.13908 (2018).

12 Szczepaniak, J., Press, C. & Kleanthous, C. The multifarious roles of Tol-Pal in Gram-negative bacteria. FEMS Microbiology Reviews 44, 490-506, doi:10.1093/femsre/fuaa018 (2020).

13 Ratliff, A. C., Buchanan, S. K. & Celia, H. Ton motor complexes. Current Opinion in Structural Biology 67, 95-100, doi:https://doi.org/10.1016/j.sbi.2020.09.014 (2021).

14 Jakes, K. S. & Cramer, W. A. Border Crossings: Colicins and Transporters. Annual Review of Genetics 46, 209-231, doi:10.1146/annurev-genet-110711-155427 (2012).

15 Housden, N. G. et al. Intrinsically disordered protein threads through the bacterial outer-membrane porin OmpF. Science 340, 1570-1574 (2013).

16 Cramer, W. A., Sharma, O. & Zakharov, S. D. On mechanisms of colicin import: the outer membrane quandary. Biochemical Journal 475, 3903-3915, doi:10.1042/bcj20180477 (2018).

17 Arima, K., Katoh, Y. & Beppu, T. Studies on Colicin B: Mode of Action and New Extraction Method from Cells. Agricultural and Biological Chemistry 32, 170-177, doi:10.1080/00021369.1968.10859043 (1968).

18 Devanathan, S. & Postle, K. Studies on colicin B translocation: FepA is gated by TonB. Molecular Microbiology 65, 441-453, doi:https://doi.org/10.1111/j.1365-2958.2007.05808.x (2007).

19 Pressler, U., Braun, V., Wittmann-Liebold, B. & Benz, R. Structural and functional properties of colicin B. Journal of Biological Chemistry 261, 2654-2659, doi:https://doi.org/10.1016/S0021-9258(17)35837-4 (1986).

20 Buchanan, S. K. et al. Crystal structure of the outer membrane active transporter FepA from Escherichia coli. Nature Structural Biology 6, 56-63, doi:10.1038/4931 (1999).

21 Dhar, R. & Slusky, J. S. Outer membrane protein evolution. Current Opinion in Structural Biology 68, 122-128 (2021).

22 Franklin, M. W. et al. Evolutionary pathways of repeat protein topology in bacterial outer membrane proteins. Elife 7, e40308 (2018).

23 Jakes, K. S. & Finkelstein, A. The colicin Ia receptor, Cir, is also the translocator for colicin Ia. Molecular microbiology 75, 567-578 (2010).

24 Payne, M. A. et al. Biphasic Binding Kinetics between FepA and Its Ligands*. Journal of Biological Chemistry 272, 21950-21955, doi:https://doi.org/10.1074/jbc.272.35.21950 (1997).

25 Tamm, L. K., Hong, H. & Liang, B. Folding and assembly of β-barrel membrane proteins. Biochimica et Biophysica Acta (BBA) - Biomembranes 1666, 250-263, doi:https://doi.org/10.1016/j.bbamem.2004.06.011 (2004).

26 Sharp, C., Bray, J., Housden, N. G., Maiden, M. C. J. & Kleanthous, C. Diversity and distribution of nuclease bacteriocins in bacterial genomes revealed using Hidden Markov Models. PLOS Computational Biology 13, e1005652, doi:10.1371/journal.pcbi.1005652 (2017).

27 Cao, Z. & Klebba, P. E. Mechanisms of colicin binding and transport through outer membrane porins. Biochimie 84, 399-412, doi:https://doi.org/10.1016/S0300-9084(02)01455-4 (2002).

28 Wookey, P. & Rosenberg, H. Involvement of inner and outer membrane components in the transport of iron and in colicin B action in Escherichia coli. Journal of Bacteriology 133, 661-666 (1978).

29 Hilsenbeck, J. L. et al. Crystal structure of the cytotoxic bacterial protein colicin B at 2.5 Å resolution. Molecular Microbiology 51, 711-720, doi:https://doi.org/10.1111/j.1365-2958.2003.03884.x (2004).

30 Harmalkar, A. & Gray, J. J. Advances to tackle backbone flexibility in protein docking. Current Opinion in Structural Biology 67, 178-186 (2021).

31 Cheng, Y.-S. et al. High-resolution Crystal Structure of a Truncated ColE7 Translocation Domain: Implications for Colicin Transport Across Membranes. Journal of Molecular Biology 356, 22-31, doi:https://doi.org/10.1016/j.jmb.2005.11.056 (2006).

32 Dormán, G., Nakamura, H., Pulsipher, A. & Prestwich, G. D. The Life of Pi Star: Exploring the Exciting and Forbidden Worlds of the Benzophenone Photophore. Chem Rev 116, 15284-15398, doi:10.1021/acs.chemrev.6b00342 (2016).

33 White, P. et al. Exploitation of an iron transporter for bacterial protein antibiotic import. Proceedings of the National Academy of Sciences 114, 12051-12056, doi:10.1073/pnas.1713741114 (2017).

34 Leman, J. K. et al. Macromolecular modeling and design in Rosetta: recent methods and frameworks. Nature methods 17, 665-680 (2020).

35 Smallwood, C. R. et al. Concerted loop motion triggers induced fit of FepA to ferric enterobactin. Journal of General Physiology 144, 71-80 (2014).

36 Newton, S. M., Igo, J. D., Scott, D. C. & Klebba, P. E. Effect of loop deletions on the binding and transport of ferric enterobactin by FepA. Molecular microbiology 32, 1153-1165 (1999).

37 Scott, D. C., Newton, S. M. & Klebba, P. E. Surface loop motion in FepA. Journal of bacteriology 184, 4906-4911 (2002).

38 Ma, L. et al. Evidence of ball-and-chain transport of ferric enterobactin through FepA. Journal of Biological Chemistry 282, 397-406 (2007).

39 Smallwood, C. R. et al. Fluoresceination of FepA during colicin B killing: effects of temperature, toxin and TonB. Molecular Microbiology 72, 1171-1180, doi:https://doi.org/10.1111/j.1365-2958.2009.06715.x (2009).

40 Schramm, E., Mende, J., Braun, V. & Kamp, R. M. Nucleotide sequence of the colicin B activity gene cba: consensus pentapeptide among TonB-dependent colicins and receptors. Journal of Bacteriology 169, 3350-3357, doi:10.1128/jb.169.7.3350-3357.1987 (1987).

41 Mende, J. & Braun, V. Import-defective colicin B derivatives mutated in the TonB box. Molecular Microbiology 4, 1523-1533, doi:https://doi.org/10.1111/j.1365-2958.1990.tb02063.x (1990).

42 Hickman, S. J., Cooper, R. E. M., Bellucci, L., Paci, E. & Brockwell, D. J. Gating of TonB-dependent transporters by substrate-specific forced remodelling. Nature Communications 8, 14804, doi:10.1038/ncomms14804 (2017).

43 Ghai, I. & Ghai, S. Understanding antibiotic resistance via outer membrane permeability. Infection and drug resistance 11, 523 (2018).

44 Górska, A., Sloderbach, A. & Marszałł, M. P. Siderophore–drug complexes: potential medicinal applications of the 'Trojan horse'strategy. Trends in pharmacological sciences 35, 442-449 (2014).

45 Kong, H. et al. An overview of recent progress in siderophore-antibiotic conjugates. European Journal of Medicinal Chemistry 182, 111615, doi:https://doi.org/10.1016/j.ejmech.2019.111615 (2019).

46 Rabsch, W. et al. FepA-and TonB-dependent bacteriophage H8: receptor binding and genomic sequence. Journal of bacteriology 189, 5658-5674 (2007).

47 Khait, R. & Schreiber, G. FRETex: a FRET-based, high-throughput technique to analyze protein–protein interactions. Protein Engineering Design and Selection 25, 681-687 (2012).

48 Housden, N. G. et al. Directed epitope delivery across the Escherichia coli outer membrane through the porin OmpF. Proceedings of the National Academy of Sciences 107, 21412-21417, doi:10.1073/pnas.1010780107 (2010).

49 Kleanthous, C., Rassam, P. & Baumann, C. G. Protein–protein interactions and the spatiotemporal dynamics of bacterial outer membrane proteins. Current Opinion in Structural Biology 35, 109-115, doi:https://doi.org/10.1016/j.sbi.2015.10.007 (2015).

50 Hernandez, H. & Robinson, C. V. Determining the stoichiometry and interactions of macromolecular assemblies from mass spectrometry. Nature protocols 2, 715-726 (2007).

51 Yang, B. et al. Identification of cross-linked peptides from complex samples. Nature Methods 9, 904-906, doi:10.1038/nmeth.2099 (2012).

52 Webb, B. & Sali, A. Comparative protein structure modeling using MODELLER. Current protocols in bioinformatics 54, 5.6. 1-5.6. 37 (2016).

53 Conway, P., Tyka, M. D., DiMaio, F., Konerding, D. E. & Baker, D. Relaxation of backbone bond geometry improves protein energy landscape modeling. Protein Science 23, 47-55 (2014).

54 Zhang, Z. & Lange, O. F. Replica exchange improves sampling in low-resolution docking stage of RosettaDock. PLoS One 8, e72096 (2013).

55 Zhang, Z., Schindler, C. E., Lange, O. F. & Zacharias, M. Application of enhanced sampling Monte Carlo methods for high-resolution protein-protein docking in Rosetta. PLoS One 10, e0125941 (2015).

56 Marze, N. A., Roy Burman, S. S., Sheffler, W. & Gray, J. J. Efficient flexible backbone protein–protein docking for challenging targets. Bioinformatics 34, 3461-3469 (2018).

57 Smith, C. A. & Kortemme, T. Backrub-like backbone simulation recapitulates natural protein conformational variability and improves mutant side-chain prediction. Journal of molecular biology 380, 742-756 (2008).

58 Kleiger, G., Saha, A., Lewis, S., Kuhlman, B. & Deshaies, R. J. Rapid E2-E3 assembly and disassembly enable processive ubiquitylation of cullin-RING ubiquitin ligase substrates. Cell 139, 957-968 (2009).

Figures

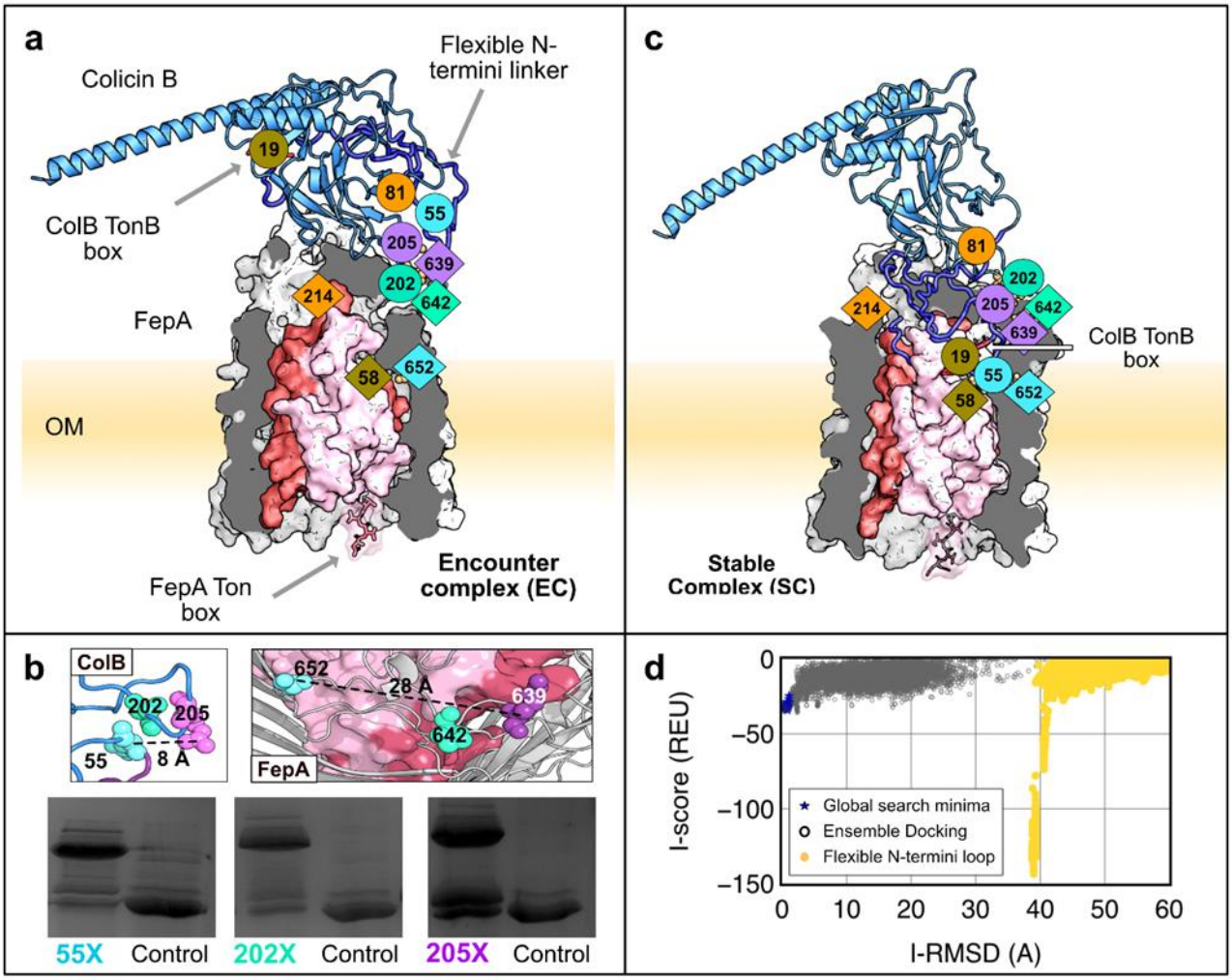

Fig. 1| Structural insights on the ColB-FepA complex by pBPA crosslinking and Rosetta-based structural modeling a. Initial encounter complex (EC) modeled with moderate to little backbone flexibility (under 5 Å RMSD). ColB (blue) and FepA (grey) form this encounter complex with *in vitro* crosslinks, FepA-K639 and ColB-D202 (teal), and FepA-P642 and ColB-R205 (purple), which lie in proximity in the model. The last *in vitro* crosslink pair, FepA-S652 and ColB-Q55 (cyan), and the two *in vivo* crosslinks, FepA-T58 and ColB-M19 (olive), and FepA A214 and ColB-G81 (orange), are not satisfied in this structure. **b.** Mapped *in vitro* crosslinking sites on the ColB and FepA PDB structures (1RH1 and 1FEP respectively). Cropped relevant crosslinks gels. Self-crosslinking control to the right of each lane (full *in vitro* crosslinking image at Extended data Fig. 3a). **c.** Fully assembled spontaneously formed stable complex (SC) modeled with the Rosetta FlopyTail algorithm[58] stimulating the partially unstructured ColB 1-55 as a floppy-tail. **d.** Rosetta Interface score vs Interface RMSD for output structures identified by local docking (ReplicaDock2) of ColB to FepA. RMSD is measured relative to the lowest-scoring global docking structure. There is a deep minima resulting from the arrangement of the flexible N-linker for the FloppyTail models.

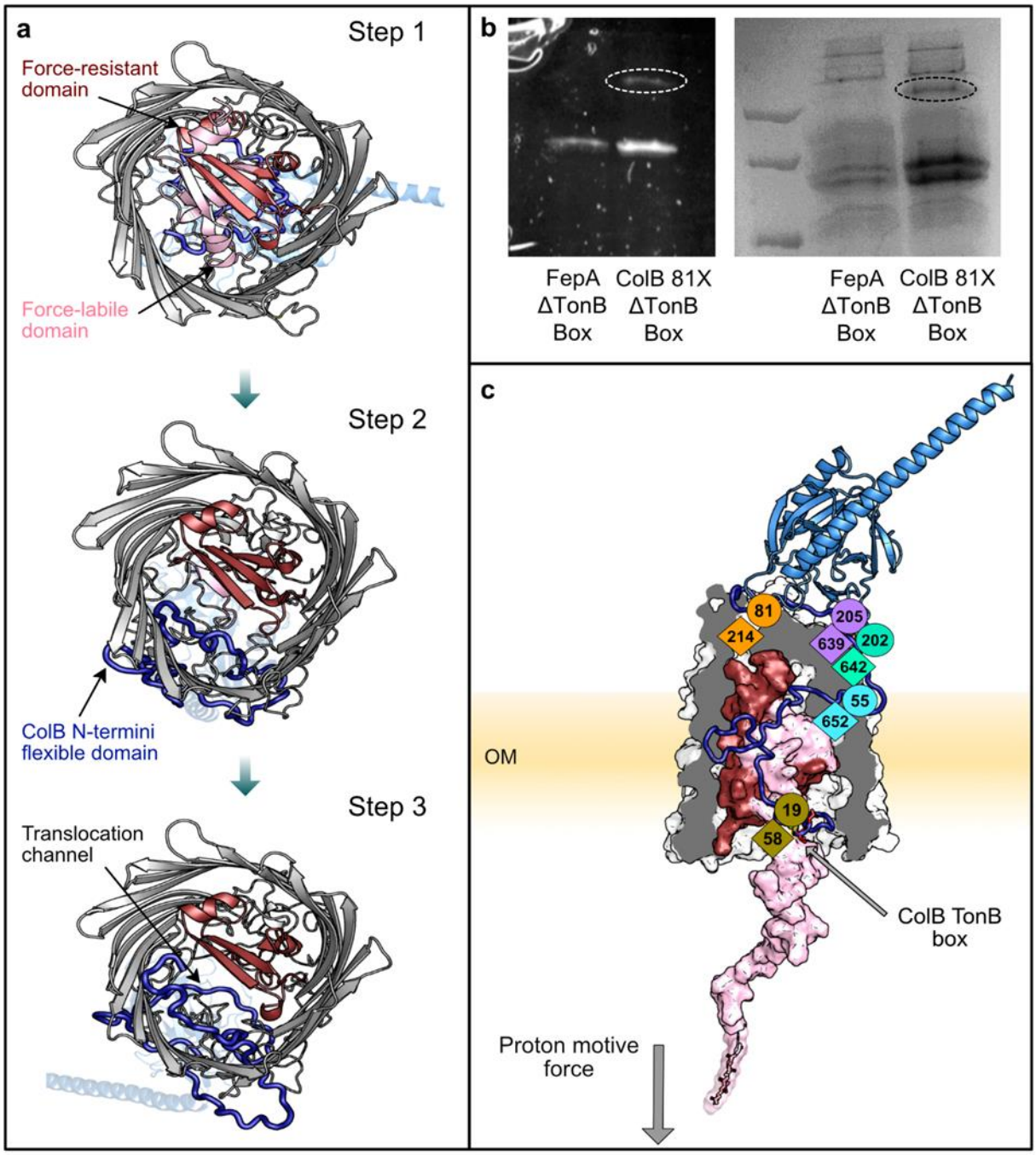

Fig. 2| The partially unstructured N-terminal ColB RT tail occupies the gap generated by the active unfolding of the FepA N-terminal half plug domain. a. A bottom-to-top view of the hypothesized translocation pathway (Stage 3) created with Rosetta by pulling the FepA N-terminus into the cell. Step 1: SC complex is formed and the force-labile half-plug domain (light pink) begins to unfold. Step 2: The force-labile half-plug is partially unfolded which allows the ColB N-terminal loop (blue) to occupy the void created by the absence of the plug domain. Step 3: The unfolding of the FepA half-plug domain creates a channel for the ColB N-terminal loop to enter. b. The ability of ColB-81X GFP to crosslink *in vivo* as a function of both ColB and FepA TonB boxes. GFP fluorescence (right) Coomassie blue stain (left). Crosslinked band circled. c. The top-scoring model portraying the translocon state (Step 3). In this final-stage model, all the crosslink constraints are satisfied and the model is energetically favorable over other states.

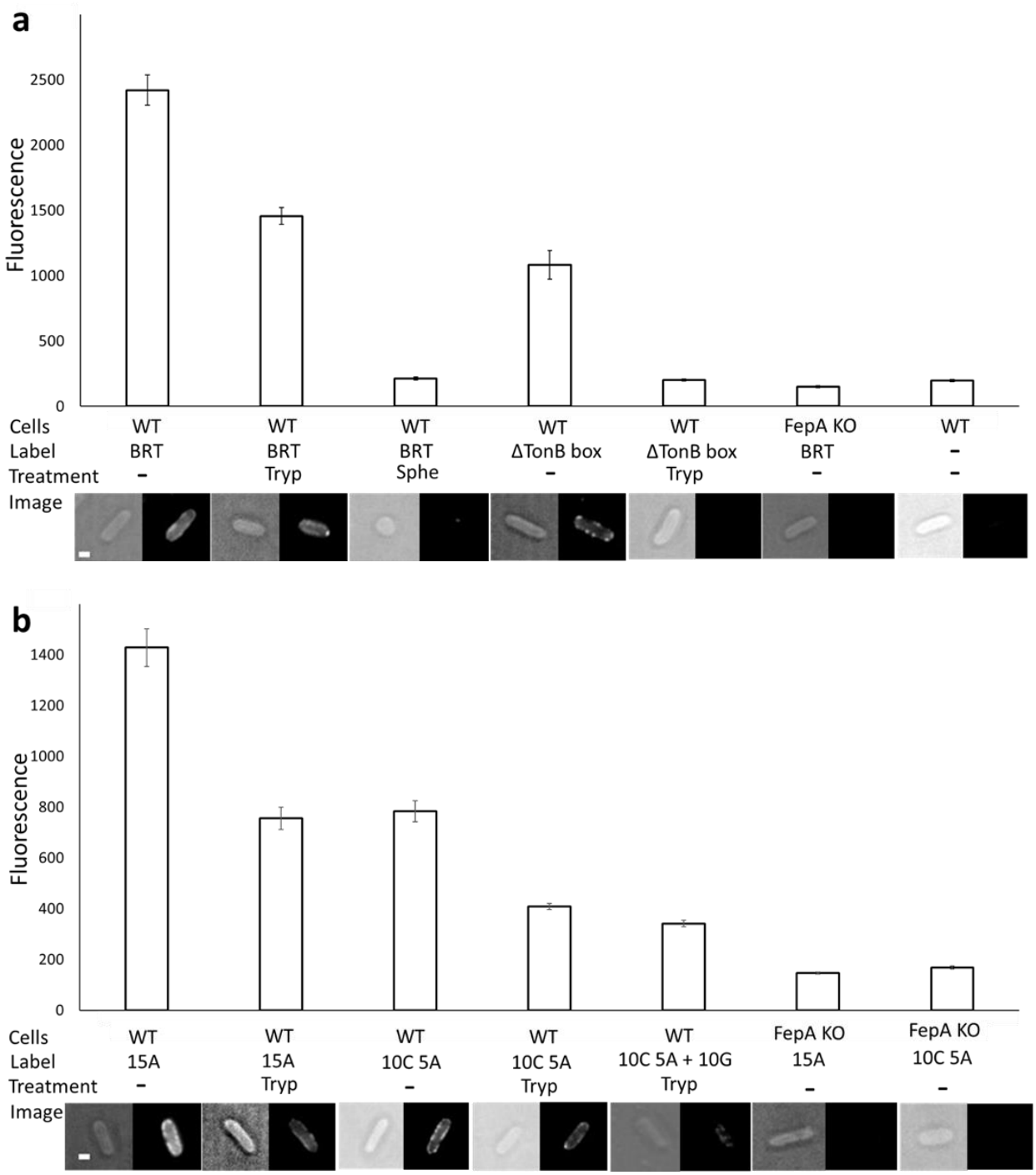

Fig. 3| ssDNA follows the ColB RT translocation path into *E. coli* cells. a. Translocation of ColB RT-Alexa 488 (BRT) or ColB RT ΔTonB box – Alexa 488 (ΔTonB box) constructs into *E. coli* MC1655 cells (WT) or *E. coli* BW25113 ΔFepA (FepA KO) cells grown in minimal media to mid log growth phase (OD_{600}~0.35). Cellular translocation defined as fluorescent signal resistant to trypsin treatment (Tryp). Cytoplasmic localization defined as fluorescent signal remaining after spheroplasting the cells, which results in the removal of the OM and the periplasmic peptidoglycan layer (Sphe). The averaged fluorescence intensities were calculated from at least 120 cells (30 cells x 4 biological repeats), standard error bars of each treatment are shown. Representative cellular images below each treatment. Scale bar – 1 µm. **b.** Translocation of ColB RT-DNA fused constructs: ColB RT-15A Alexa 488 (15A), ColB RT 10C 5A Alexa 488 (10C 5A), ColB RT 10C 5A Alexa 488 + 10G (10C 5A + 10G).